Nuclear Instruments and Methods in Physics Research A 807 (2016) 86–93

Contents lists available at ScienceDirect

Nuclear Instruments and Methods in Physics Research A

journal homepage: www.elsevier.com/locate/nima

Design of a compact Faraday cup for low energy, low intensity ion beams

E.D. Cantero [a,*], A. Sosa [a,b], W. Andreazza [a], E. Bravin [a], D. Lanaia [a], D. Voulot [a], C.P. Welsch [b,c]

[a] CERN, 1211 Geneva 23, Switzerland
[b] The University of Liverpool, Liverpool, United Kingdom
[c] The Cockcroft Institute, Sci-Tech Daresbury, Daresbury, Warrington, United Kingdom

ARTICLE INFO

Article history:
Received 3 June 2015
Received in revised form
26 August 2015
Accepted 28 September 2015
Available online 4 November 2015

Keywords:
Faraday cup
Beam diagnostics
Ion beam currents
HIE-ISOLDE

ABSTRACT

Beam intensity is one of the key parameters in particle accelerators, in particular during machine commissioning, but also during operation for experiments. At low beam energies and low intensities a number of challenges arise in its measurement as commonly used non-invasive devices are no longer sensitive enough. It then becomes necessary to stop the beam in order to measure its absolute intensity. A very compact Faraday cup for determining ion beam currents from a few nanoamperes down to picoamperes for the HIE-ISOLDE post-accelerator at CERN has been designed, built and tested with beam. It has a large aperture diameter of 30 mm and a total length of only 16 mm, making it one of the most compact designs ever used.

In this paper we present the different steps that were involved in the design and optimization of this device, including beam tests with two early prototypes and the final monitor. We also present an analysis of the losses caused by secondary particle emission for different repelling electrode voltages and beam energies. Finally, we show that results obtained from an analytical model for electron loss probability combined with Monte Carlo simulations of particles trajectories provide a very good agreement with experimental data.

1. Introduction

Faraday cups (FCs) are instruments used in particle accelerators to determine the instantaneous current of a beam of charged particles. The working principle consists of intercepting the beam with a metallic electrode (known as collector or signal cup) where the projectiles are stopped, and reading the rate of deposited charge by means of a sensitive ammeter. The emission of secondary charges from the electrode may lead to an unwanted signal that would falsify the absolute beam current determination. Typical mechanisms introduced to reduce the loss of charges include the construction of the collector as a deep cup-shaped electrode (large length to aperture ratio) and the application of electric (and sometimes also magnetic) fields to prevent the loss of the secondary charges [1,2].

In this work we present the studies corresponding to the design of a compact FC that will be used as a current monitor for the superconducting linac and beam transfer lines of the HIE-ISOLDE [3,4] post-accelerator at CERN. The (pulsed) beams to be measured will be composed of light to medium ions (from He to Ar) in the energy range from 0.3 to 10 MeV/u, and with average currents in the order of several pA to a few nA [5]. The maximum expected range of those particles in the collector is below 300 μm, and the beam power is low enough (less than 0.5 W) that no active cooling of the collector is needed.

The use of FCs in particle accelerators is in most cases restricted to relative measurements of beam current at different locations that are used to calculate transmission factors. The scenario is much complex at HIE-ISOLDE, in particular along the linac where many beam parameters like energy, longitudinal and transverse profiles are substantially changed and as a result absolute measurements of total beam currents are needed. The motivation for this work is given by a critical constraint on the FC geometry due to limitations on the longitudinal space available for diagnostics in the linac region of the HIE-ISOLDE post-accelerator. An overall longitudinal distance of 220 mm between the flanges of cryomodules is shared among vacuum valves, a steering magnet and the diagnostic box. A maximum longitudinal length of only 16 mm were allocated for the FC, which has an aperture diameter of 30 mm (typical beam sizes are of the order of 5 mm FWHM). As a consequence, the collector cannot have the typical deep cup-shape geometry and all the distances and thicknesses of the internal parts of the FC need to be carefully considered and optimized in order to control the emission of secondary particles. More details about the HIE-ISOLDE beam diagnostic system and its main features can be found elsewhere [5].

* Corresponding author.
E-mail address: esteban.cantero@cern.ch (E.D. Cantero).

http://dx.doi.org/10.1016/j.nima.2015.09.096
0168-9002/

The structure of this paper is as follows: In Section 2 we analyse a typical Faraday cup, which was used as a starting point for the design of the compact FC. After that, three different compact FC designs are presented (including two prototypes and the final design for the HIE-ISOLDE compact FC) and their main features are discussed. A model for the electron loss from the cups including particle-tracking simulations is presented in Section 4. Results of experimental tests of the FCs with beam and comparisons with simulation are discussed in Section 5, followed by conclusions in Section 6.

2. Analysis of a typical Faraday cup design

Beam current measurements using a FC can be affected by several possible sources of systematic errors. One of them is the loss of ion-induced secondary electrons that are emitted with energies higher than the electrostatic potential barrier and escape from the cup. The total yield of secondary electron emission and its energy spectrum is highly dependent not only on the projectile type and incident energy, but also on the material chosen for the collector and the condition of its surface. In general the secondary electron energy spectrum presents a peak at an energy E_{max} below 10 eV and has a long decaying tail for higher energies [6,7]. Another possible cause of errors is the backscattering of electrons that are bound to the incoming ions when they are not fully stripped. If these electrons are elastically backscattered they can overcome the potential barrier leading to a loss of negative charge. The cross-section of this phenomenon scales with the target atomic number and is usually very small, so this effect can normally be neglected. Another unwanted systematic error in the measurement comes from any leakage currents between the repeller and the collector, which results in an offset current. To simplify the design of the insulators and also to reduce the amount of leakage currents in the cup, a maximum absolute value of 500 V was chosen for the repeller bias voltage.

Fig. 1a shows the layout of a typical FC used in the REX-ISOLDE accelerator at CERN [8]. This cup has a standard design and is used to monitor low energy (below 3 MeV/u) ion beams. The aperture is 26 mm, the collector has an internal radius r of 15 mm and a longitudinal length l of 32 mm. The design of the collector with a large l/r ratio prevents the escape of most of the emitted secondary charges, even in the absence of electric fields, by what we call the geometrical capture effect. Secondary particles emitted and recaptured by the collector do not alter the net current monitored by the ammeter and hence have no influence on the measurement. This effect is enhanced as the solid angle formed from the centre of the collector to its extremities is reduced (i.e. increasing l/r). In order to avoid the loss of low energy secondary electrons that are not recaptured on the collector walls a potential barrier is introduced by adding a repeller to the cup extremity operating at a bias voltage of -60 to -100 V. A plot of the equipotential surfaces in the cup for an applied repelling voltage of $V_{rep} = -100$ V is shown in Fig. 1b. The minimum height of the potential barrier is located along the cup axis, where it reaches a maximum value of 61 eV.

For the FC and ion beam parameters of HIE-ISOLDE the systematic error produced by the backscattering of electrons originally bound to the incoming projectiles and by leakage currents were determined to be within the experimental resolution of 1% by measuring beam currents for different charge states and repeller voltages, and were therefore considered as negligible. The effect of high-energy electron backscattering can be much larger when considering an incident beam of negative ions, due to the low binding energy of the external electron. In that case the effect of electron backscattering cannot be neglected. The most critical point involved in the design of the required compact FC for measuring the HIE-ISOLDE ion beams is the loss of (ion-induced) secondary electrons. A careful design of all the internal parts of the FC is required to properly address this issue, which is described in the following section.

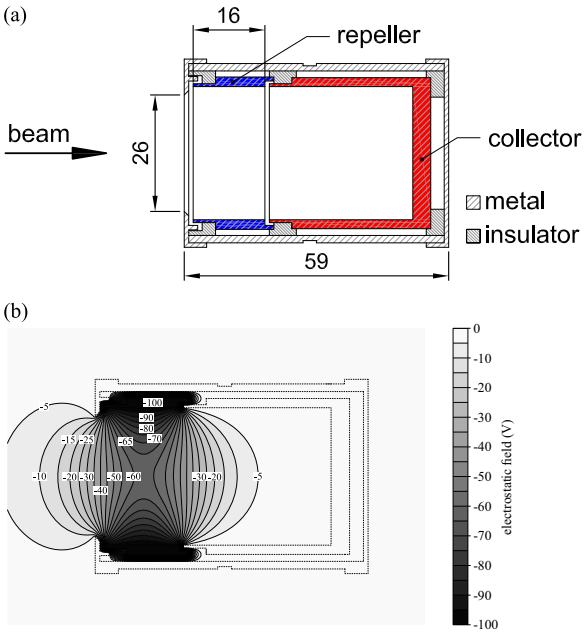

Fig. 1. Standard Faraday cup used in REX-ISOLDE. (a) Cross section view of the standard REX-ISOLDE Faraday cup. Distances in mm. The metallic parts are made of stainless steel and the insulators are made of Vespel®. (b) Contour plot of the electrostatic potential field with $V_{rep} = -100$ V. The potential barrier height is 61 eV for electrons moving along the axis of the cup.

3. Optimization of the geometry of the compact Faraday cup

The main goal of the geometry optimization was to obtain a reliable FC for HIE-ISOLDE that would fit in the small space available for beam instrumentation devices between the cryomodules of the superconducting linac (16 mm of total longitudinal length). The most important constraints were the maximum repelling voltage allowed and the efficiency of re-capturing the low-energy secondary electrons, which is directly correlated with the minimum height of the potential barrier, as is detailed below. The characteristics of the typical REX-ISOLDE FC were taken as a starting point in the process of designing the first prototype of such a compact FC (Prototype 1) shown in Fig. 2.

The longitudinal extension of the collector was reduced to a minimum, leading to a plane electrode with no walls to retain secondary electrons. With the imposed constraints in the longitudinal dimension of the FC, the efficiency for retaining the particles with the geometrical capture effect is very low. The repeller cylinder was reduced in the longitudinal direction into a ring of 1.5 mm length, an order of magnitude shorter than the typical value. As the effectiveness for retaining secondary particles is clearly reduced in this design, a higher value for the repelling voltage was foreseen, with $V_{rep} = -500$ V. The electrostatic potential field of this cup is shown in Fig. 2b. It is important to note that even with this substantial increase in V_{rep} the potential barrier is still 38% lower than that obtained with the original REX-ISOLDE FC of Fig. 1. To reduce the possibility of having leakage currents between the repeller and collector, a grounded metallic guard ring was installed between them. Experimental tests with beam on this prototype (presented in the following section) showed that this design did not reach the specifications and

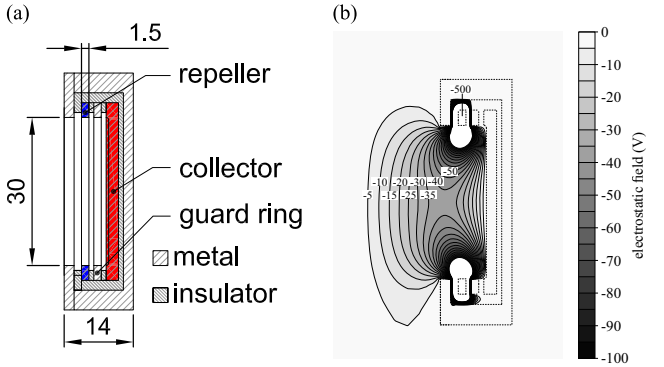

Fig. 2. Prototype 1 for the HIE-ISOLDE compact Faraday cup. (a) Cross-section view of the Faraday cup. Distances in mm. The metallic parts are made of stainless steel and the insulators are made of Vespel®. (b) Contour plot of the electrostatic potential field with $V_{rep} = -500$ V. The potential barrier height is 38 eV for electrons moving along the axis of the cup.

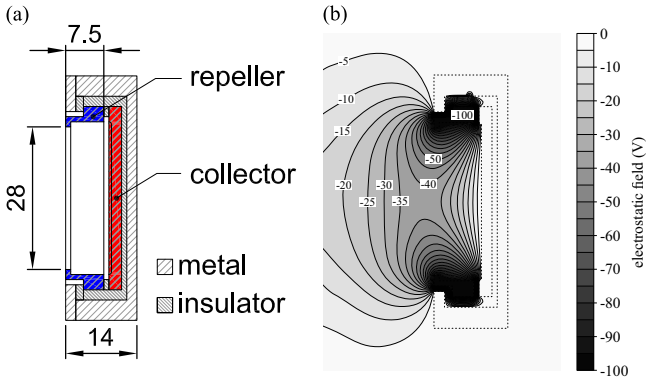

Fig. 3. Prototype 2 for the HIE-ISOLDE compact Faraday cup. (a) Cross-section view of the Faraday cup. Distances in mm. The collector and the repeller are made of aluminium, the FC body is made of stainless steel and the insulators are made of Vespel®. (b) Contour plot of the electrostatic potential field with $V_{rep} = -100$ V. The potential barrier height is 39 eV for electrons moving along the axis of the cup.

therefore a second prototype (Prototype 2) was built. A layout of its design is presented in Fig. 3.

Prototype 2 was implemented using the main structure of Prototype 1, with changes in the internal parts of the cup based on results obtained from numerical simulations of the electrostatic potential fields. It does not include a guard ring, allowing the longitudinal extension of the repeller to be increased. The FC aperture is defined by the repeller itself and not by the external aperture off the FC body. The dimensions of the collector remain unchanged from the previous prototype, but both the repeller and the collector are made from aluminium rather than stainless steel. The reason underlying this change in materials is the reduction in the probability for backscattering of the incoming ions [9]. With the extended repeller length, the on-axis electrostatic potential barrier reaches a maximum of 39 eV for a repelling voltage of $V_{rep} = -100$ V, a similar value to that obtained in Prototype 1 for $V_{rep} = -500$ V. Having a lower repeller voltage reduces leakage currents as they are proportional to V_{rep}. Note also that the variation of the electrostatic potential in the radial direction is much lower in prototype 2 than in prototype 1, therefore unwanted radial components of the electric field are reduced in this version of the compact FC.

The final design of the compact Faraday cup is presented in Fig. 4. It is an optimized version of Prototype 2, with minor adaptations of the thickness of the internal parts in order to maximize the longitudinal extension of the repeller. In this version

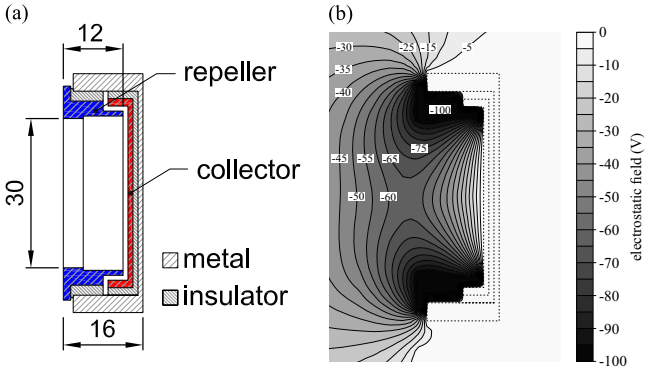

Fig. 4. Final design of the HIE-ISOLDE compact Faraday cup. (a) Cross-section view of the Faraday cup. Distances in mm. The collector and the repeller are made of aluminium, the FC body is made of stainless steel and the insulators are made of Vespel® . (b) Contour plot of the electrostatic potential field with $V_{rep} = -100$ V. The potential barrier height is 63 eV for electrons moving along the axis of the cup.

Table 1
Summary of the main parameters of the Faraday cups. l and r are the repeller length and radius, respectively, and U is the potential barrier height for $V_{rep} = -100$ V.

FC	l (mm)	r (mm)	U (eV)	Collector material
REX-ISOLDE	16.0	13.0	61	Stainless steel
Prototype 1	1.5	15.0	8	Aluminium
Prototype 2	7.5	14.0	39	Aluminium
HIE-ISOLDE final design	12.0	15.0	63	Aluminium

both the repeller and the collector are separated from the FC body by Vespel® insulators, with the aim of further reducing the residual conductivity between them to minimise leakage currents. The maximum on-axis potential barrier height of this cup for a repelling voltage of $V_{rep} = -100$ V is 63 eV.

In Table 1 we summarize the main parameters of the different FC models. An analysis of the secondary electron loss contribution on the measurement of beam currents is proposed in the following section, based on probabilities of recapturing such electrons determined with Monte Carlo simulations.

4. Electron loss model

In order to study the effects of electron loss for different FCs and applied repeller voltage values, we propose the following model that considers the flow of charges collected and emitted by the repeller. It is important to note that this model does not include any particles that might be collected by the FC other than the incident beam and the secondary electrons produced by the beam when it hits the collector. This means that the contribution of tertiary charges to I_{FC} (for example from the collection of electrons emitted at the repeller after the impact of primary ions or secondary electrons) is neglected. The impact of making this assumption on our work is negligible, as the beam size is much smaller than the FC diameter. It is also assumed that all the incident ions are collected with a fixed charge state q. The inclusion of several charge states for the projectiles in the present description is straigthforward.

The current read by the FC (I_{FC}) can be considered as being the sum of the beam current (I_{beam}) and an extra component I_{loss}, which represents the combined effects of all electrons emitted and not recaptured by the collector,

$$I_{FC} = I_{beam} + I_{loss}. \quad (1)$$

For a given beam and FC with its repeller biased to V_{rep}, and assuming that the number of electrons emitted is proportional to the number of incident ions on the collector with no dependence on the charge state q of these ions, we obtain

$$\frac{I_{loss}(V_{rep})}{I_{beam}} = \frac{Y_{loss}(V_{rep})}{q}, \quad (2)$$

where Y_{loss} represents the mean number of lost electrons per incident ion. Note that this quantity depends on the ion species and its energy, the FC geometry, the applied repeller voltage and the surface condition of the collector.

Y_{loss} can be calculated as the product of the total number of emitted electrons per incident ion (Y_{tot}) and the mean probability P_{loss} of losing an emitted electron,

$$Y_{loss}(V_{rep}) = Y_{tot} P_{loss}(V_{rep}). \quad (3)$$

Moreover, we can define

$$P_{loss}(V_{rep}) = \int_0^{E'} \mathrm{dE}\ N(E)\ \eta(E, V_{rep}), \quad (4)$$

where E is the emitted electron energy, $N(E)$ represents the normalized number of secondary electrons emitted with energy E (such that $\int_0^{E'} \mathrm{dE}\ N(E) = 1$) and $\eta(E, V_{rep})$ is the mean probability of losing an electron of initial energy E for a repeller voltage of V_{rep}. The mean probability η should be interpreted as an average that includes the angular distribution of the electrons and the surface of emission of such secondary electrons (given by the spot size of the beam on the collector).

The quantity $\eta(E, V_{rep})$ can be calculated by means of particle tracking simulations for any particular FC geometry. In order to calculate the impact of lost electrons on I_{FC}, the probability η, the secondary electron spectrum $N(E)$, the total yield Y_{tot}, and the beam charge state q are required.

The angular distribution of the emitted electrons is assumed to follow a cosine law,

$$\frac{\mathrm{d}N}{\mathrm{d}\Omega}(\theta) = \left.\frac{\mathrm{d}N}{\mathrm{d}\Omega}\right|_{\theta=0} \cos(\theta), \quad (5)$$

where θ denotes the angle of emission with respect to the surface normal, following Ref. [10].

4.1. Secondary electron energy spectrum

The secondary electron energy spectrum was modelled with the following analytical expression,

$$\frac{1}{N(E)} = \alpha\left(\frac{1}{E} + \frac{1}{\beta E^{-\gamma}}\right), \quad (6)$$

with $N(E)$ the normalized secondary electron spectrum, E the energy in eV, and α a normalization constant such that $\int_0^{E'} \mathrm{dE}\ N(E) = 1$, with $E' = 500$ eV. β and γ are free parameters used to shape the secondary electron spectrum. For very low energies the probability of emitting an electron with a given energy scales linearly with the energy E of the emitted electrons, while for higher energies the probability decays following a power law, $E^{-\gamma}$. The power law decay is based on an approximation proposed in Ref. [6]. The value of β determines the crossover point between these two regimes and hence the energy of the maximum in the spectrum. It is common to describe the electron spectrum in terms of the position of the maximum E_{max} and the half-width of the distribution, $\Delta_{1/2}$.

The values of β and γ were chosen so as to give the best agreement between the simulations and the present experimental results. The energy spectrum considered in this work for the stainless steel collectors (REX-ISOLDE FC and prototype 1) was generated with the parameters $\beta^{s.s.} = 0.5$ and $\gamma^{s.s.} = 1.3$, which results in $E^{s.s.}_{max} = 0.7$ eV and $\Delta^{s.s}_{1/2} = 1.8$ eV. For the aluminium collectors (prototype 2 and final design), the values are $\beta^{Al} = 1.0$, $\gamma^{Al} = 1.5$, resulting in $E^{Al}_{max} = 0.9$ eV and $\Delta^{Al}_{1/2} = 2.0$ eV. Both spectra are shown in Fig. 5.

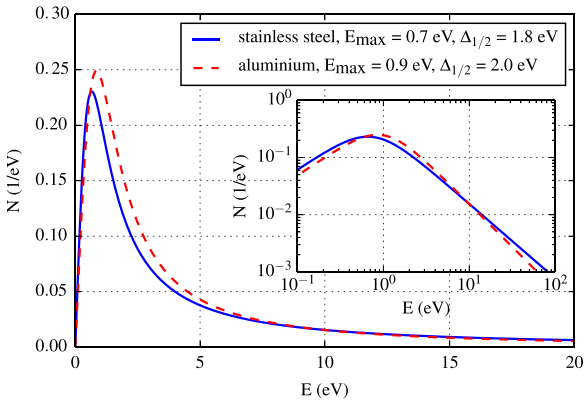

Fig. 5. Normalized energy spectra for secondary electron emission used in this work for the stainless steel and aluminium collectors. The inset shows the same spectra on a logarithmic scale.

4.2. Incident charge state and total emission yield

The beam used for the experimental tests of the REX-ISOLDE FC and prototypes 1 and 2 was mostly $^{20}Ne^{5+}$, giving the impacting ions an incident charge state of $q = 5$. As it was not possible to experimentally determine the secondary electron yield of stainless steel and aluminum for such ions, the total yield Y_{tot} was taken to be a free parameter when fitting the simulation to the present experimental results. The best agreement was obtained with the values $Y^{s.s.}_{tot} = 15$ electrons/ion for the stainless steel collectors, and $Y^{Al}_{tot} = 8.5$ electrons/ion for the aluminium collectors.

For the measurements performed at ISAC II (TRIUMF) on the final design of the compact FC with an aluminum collector, $^{4}He^{+}$ and $^{20}Ne^{5+}$ beams were used, leading to impacting ions with charge states $q = 1$ and $q = 5$ respectively. Comparing simulations to experimental results confirmed $Y^{Al}_{tot} = 8.5$ electrons/ion for $^{20}Ne^{5+}$. The data obtained with the $^{4}He^{+}$ beam did not differ significantly from that of $^{20}Ne^{5+}$ and as a consequence a value of $Y^{Al}_{tot} = 8.5/5 = 1.7$ electrons/ion was adopted for $^{4}He^{+}$.

4.3. Probability of losing the emitted electrons as a function of energy and applied repeller voltage

The values of $\eta(E, V_{rep})$ were determined using CST Particle Studio™ [11]. Electrons were simulated as being emitted from a circular source equivalent in size to the beam spot centered on the collector with the cosine angular distribution mentioned previously. For each repeller voltage V_{rep}, the trajectories of $n_{emitted} = 10,000$ electrons with an emission energy E were simulated. A fraction of these electrons ($n_{captured}$) are deflected by the electric field and return to the collector, while the remaining electrons ($n_{lost} = n_{emitted} - n_{captured}$) either overcome the potential barrier and escape from the cup or hit other internal parts of the FC. The calculation of η for each energy is then simply

$$\eta = \frac{n_{lost}}{n_{emitted}}. \quad (7)$$

Examples of simulated secondary electron trajectories using prototype 1 are presented in Fig. 6.

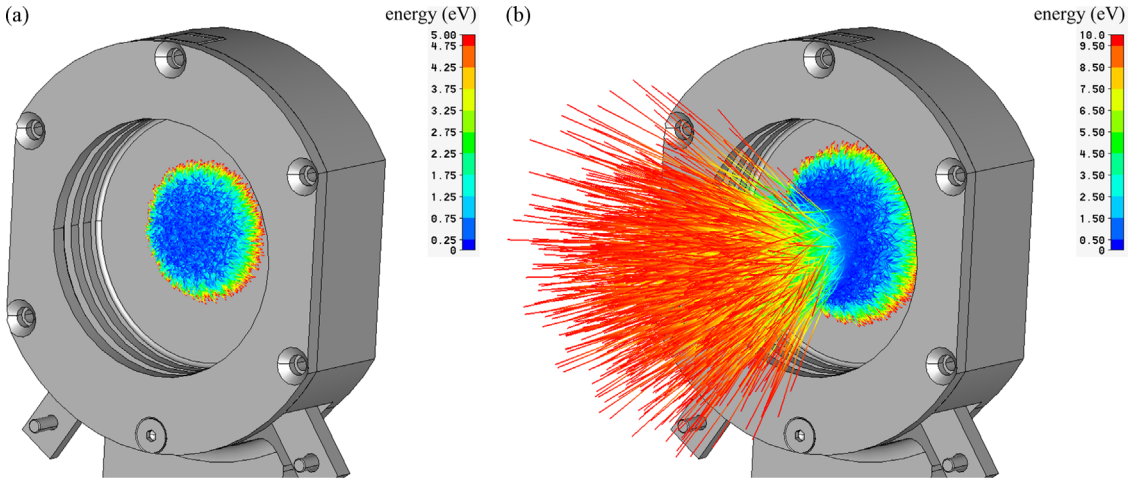

Fig. 6. Simulation of secondary electrons trajectories using Prototype 1. (a) Electrons emitted with a kinetic energy $E = 5$ eV, $V_{rep} = -100$ V. All electrons hit the collector. $\eta = 0$. (b) Electrons emitted with a kinetic energy $E = 10$ eV, $V_{rep} = -100$ V. Only a fraction of electrons hit the collector, while 15.7% of them overcome the potential barrier and leave the cup, $\eta = 0.157$.

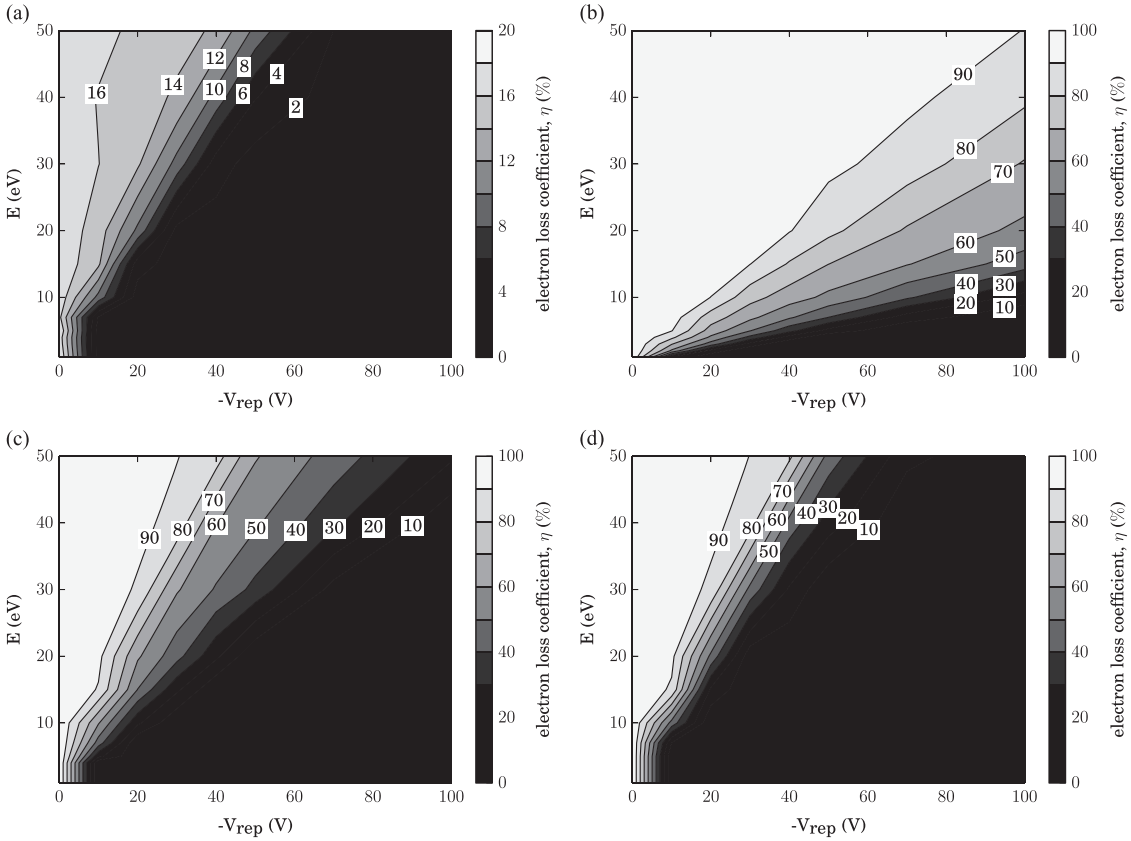

Fig. 7. Mean probability η of losing an electron emitted with an energy E while the repeller is biased to V_{rep}, based on particle tracking simulations performed with CST Particle Studio™ [11]. (a) Results for REX-ISOLDE FC. Note the different colour scale. (b) Results for prototype 1. (c) Results for prototype 2. (d) Results for final design.

4.4. Simulation results

The mean probability η of losing an electron emitted with an energy E at a repelling voltage V_{rep}, is presented in Fig. 7 for the four FC geometries studied.

It is clearly seen that the REX-ISOLDE FC, with its large length-to-aperture ratio (l/r) is very efficient, capturing over 80% of emitted electrons even with no repeller voltage (geometrical capture). For $V_{rep} = -70$ V, all electrons emitted with energies below 50 eV are collected.

For the compact cups this is not the case with close to 100% of electrons escaping when there is no repeller voltage present. The improvement in the design of the repeller in going from prototype 1 to the final design is clearly visible with the number of electrons lost with an energy of 50 eV for a repeller voltage of $V_{rep} = -100$ V decreasing from close to 100% for prototype 1 to 20% for prototype 2 with the final design achieving full capture.

By convoluting the probability of losing electrons of a given energy $\eta(E, V_{rep})$ with the normalized electron energy spectrum $N(E)$ for a given collector, the mean probability P_{loss} of losing an

emitted electron at a given V_{rep} can be calculated (Eq. (4)). Combining this with the total yield value derived in the analytical model, it was possible to calculate the dependence of the measured FC current on the repeller voltage for the four FCs, which could then be compared to the experimental results outlined in the next section.

5. Results of beam tests and comparison with simulation

Beam currents were measured with all FCs for different values of repeller voltage, in order to evaluate the quantity of secondary electrons lost. The loss of these electrons is observed as an additional current in the FC, leading to a measured current, I_{FC}, which is higher than the beam current I_{beam}. The shape of the I_{FC} vs. V_{rep} curve is mainly dependent on the secondary electron yield of the collector and energy spectrum of emitted electrons, both of which depend on the incident projectile type and its energy and can be well described by the analytical expressions derived in Section 4.

The REX-ISOLDE FC, together with the compact prototypes 1 and 2 were tested with beams from the REX-ISOLDE post-accelerator at CERN before it shut-down for the HIE-ISOLDE upgrade in March 2013. A stable (pilot) beam composed mostly of $^{20}Ne^{5+}$ was used for those measurements, with a mass to charge ratio, $A/q = 4$. The available energy range probed ranged from 0.3 to 2.8 MeV/u, with beam intensities in the order of 20–200 pA. The final design for the compact HIE-ISOLDE FC was tested with both $^{4}He^{+}$ and $^{20}Ne^{5+}$ ion beams delivered with the ISAC-II superconducting linac at TRIUMF. Here the beam energy was in the range of 1.5–5.5 MeV/u and beam intensity between 100 pA and 4 nA. The results of all the measurements are presented in Figs. 8–11.

For the three energies studied with the REX-ISOLDE FC (Fig. 8), the emission of electrons is only clearly visible as an extra current on I_{FC} when little or no repelling voltage is applied. This excess current is abruptly reduced by biasing the repeller with -50 V, with no significant change in the measured current visible from this point onwards up to $V_{rep} = -500$ V. The reference current measurement I_{beam} taken for comparison in all other measurements was therefore the current equivalent to a measurement with the REX-ISOLDE FC using a repeller bias voltage of -60 V. The experimental uncertainties present in the data are dominated by variations at the $\pm 1\%$ level in the beam current between a reference measurement of I_{beam} using the REX-ISOLDE FC and that with the FC under test.

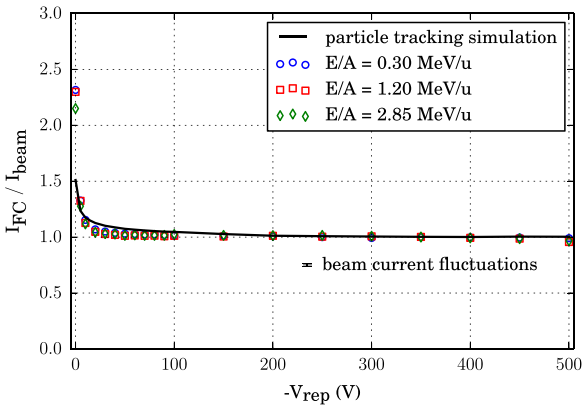

Fig. 8. Variation of the detected current I_{FC} with the repelling voltage. Beam with a mass to charge ratio of $A/q = 4$ (mostly $^{20}Ne^{5+}$). The solid line are the results of the model for electrons loss. Results for REX-ISOLDE FC, considering $Y_{tot}^{s.s.} = 15$ electrons/ion, $q = 5$ and the electron energy spectrum for stainless steel shown in Fig. 5. The reference current I_{beam} was obtained with the REX-ISOLDE FC for $V_{rep} = -60$ V.

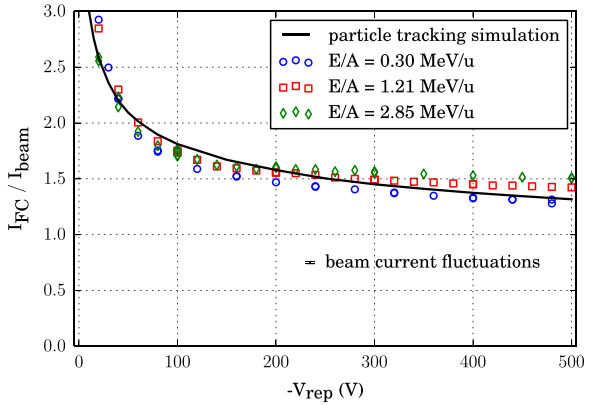

Fig. 9. Idem Fig. 8. Results for prototype 1, considering $Y_{tot}^{s.s.} = 15$ electrons/ion, $q = 5$ and the electron energy spectrum for stainless steel shown in Fig. 5. The reference current I_{beam} was obtained with the REX-ISOLDE FC for $V_{rep} = -60$ V.

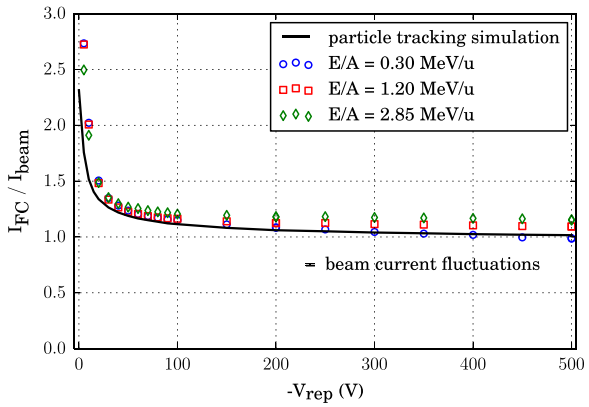

Fig. 10. Idem Fig. 8. Results for prototype 2, considering $Y_{tot}^{Al} = 8.5$ electrons/ion, $q = 5$ and the electron energy spectrum for aluminium shown in Fig. 5. The reference current I_{beam} was obtained with the REX-ISOLDE FC for $V_{rep} = -60$ V.

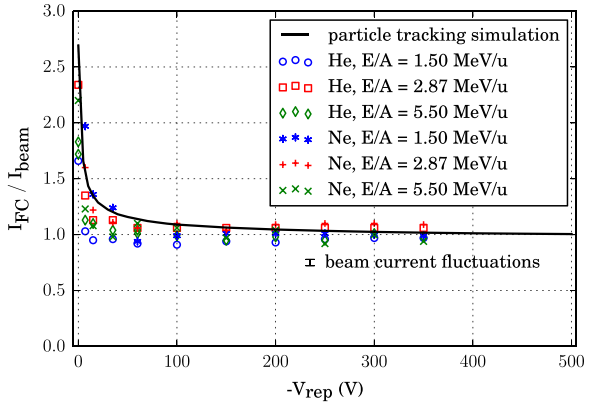

Fig. 11. Idem Fig. 8. Results for final design of the compact FC, considering the electron energy spectrum for aluminium shown in Fig. 5. For the Ne^{5+} beams, the results correspond to $Y_{tot}^{Al} = 8.5$ and $q = 5$, while for the He^{1+} beams, the results represent the case of $Y_{tot}^{Al} = 1.7$ electrons/ion and $q = 1$. The reference current I_{beam} was obtained with the REX-ISOLDE FC for $V_{rep} = -60$ V.

The results obtained with prototype 1 of the compact FC, shown in Fig. 9 are clearly seen to be non-optimal when compared to the normal behaviour of the REX-ISOLDE FC. Even at repeller voltages as high as -500 V the excess beam current measured is of the order of 30–50%. We interpret these results to be a consequence of an insufficient potential barrier leading to a high loss of secondary electrons, a

conclusion which is supported by the simulations. This initial negative result led to the extensive simulation campaign and redesign of the geometry of the compact FC, eliminating the guard ring and extending the longitudinal length of the repeller. These modifications were implemented on prototype 2.

The measurements on prototype 2 are presented in Fig. 10. The extension of the repeller length is seen to be effective in decreasing the number of secondary electrons that are lost from the collector, in agreement with simulation for the lower energy primary ions. An excess current of the order of 10–20% is nevertheless still observed for $-V_{rep} > 100$ V for higher energy primary ions, suggesting a primary ion energy dependence which is not taken into account in the analytical formulae used.

The final adaptation to the size and geometry of the internal parts of the FC essentially consisted of extending the longitudinal length of the repeller by as much as was possible, leading to the final design. The experimental results for this design are presented in Fig. 11. The data obtained show a sharp decay of the excess current read on the FC for low repeller voltages, with a plateau reached at $V_{rep} = -50$ V for all primary ion energies. On this plateau the error in the measurement is $< 10\%$, but it should be noted that the total beam current fluctuations present during the experiments performed at TRIUMF was around three times higher than that of the previous measurements performed at CERN. No clear correlation between this error and the ion species or beam energy is observable. It should, however, be noted that drifts in the beam current associated with changes in the ion source were also present during the measurements, leading to systematic offsets errors. An estimation of the effect of such drifts on the determination of I_{FC} was performed using a standard FC, and showed variations in I_{beam} of $\pm 3\%$ for time scales of the order of 1 h, similar to the time employed in acquiring each of the curves of Fig. 11. Nonetheless, the start of a plateau from $V_{rep} = -50$ V can be clearly seen. Based on these results, the final design of the compact FC will be operated with $V_{rep} = -100$ V.

Although the simple model presented in this work does not include important features of the process of ion induced electrons emission (for example, no dependence of the electrons emission yield Y_{tot} on the beam energy is considered), a qualitative good agreement is found for the calculations with respect to the experimental data in all the cases. However, it should be noted that the calculations are based on the selection of the electrons energy spectra and total yield values, that were adjusted to the experiment as no measurements of those quantities were done. At the present stage, the model for electrons emission can be considered as a good tool to describe the main features of the dependence of the FCs measurements for different repelling voltages. More complex and refined measurements and models of the electrons emission process would be required should a more detailed understanding of the results be of interest, such studies go beyond the scope of our present R & D program. Further detailed results of the calculations for different electrons energy spectra are presented in Appendix A.

6. Concluding remarks

In the context of the HIE-ISOLDE project at CERN, the design of a compact FC for measuring low-intensity ion beams currents was required. The simple adaptation of a typical FC geometry into the restricted space available proved insufficient to adequately capture the secondary electrons generated upon primary ion impact on the collector. A simulation campaign based on a simple analytical model was therefore launched to address this issue. Several prototypes were tested with beam both at REX-ISOLDE (CERN) and ISAC-II (TRIMUF) accelerators, experimentally validating a final design that meets the requirements.

A series production of six Faraday cups using the final design has been completed and these are now being installed in the HIE-ISOLDE post-accelerator at CERN. Final commissioning of all the beam diagnostic devices is scheduled to start in July 2015.

Acknowledgements

E.D.C., D.L. and A.S. acknowledge the receipt of a Marie Curie Fellowship from the European Commission under the FP7-PEOPLE-2010-ITN project CATHI (Marie Curie Actions – ITN), grant agreement No. PITN-GA-2010-264330. Collaboration of R.E. Laxdal and M. Marchetto during the measurements at TRIUMF, and advice from O.R. Jones (CERN) is gratefully acknowledged.

Appendix A. Dependence of the electron loss probability on the electron energy spectra

Four different electron energy spectra calculated with the analytical expression of Eq. (6) and shown in Fig. 12, were

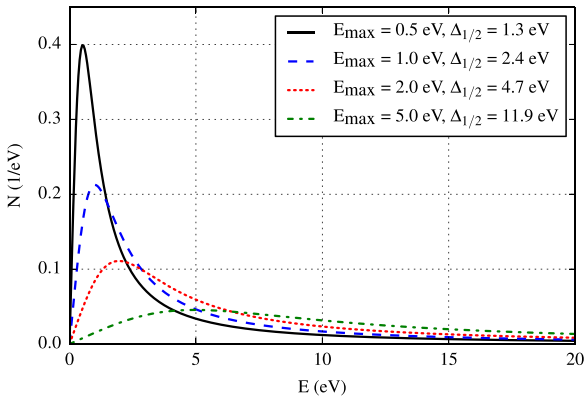

Fig. 12. Normalized energy spectra for the secondary electron emission used to characterise the dependence of the electron loss probability P_{loss} on $N(E)$. The position of the peak and the width of the distributions span over an order of magnitude for the selected examples, representing typical values for secondary electrons spectra produced by the interaction of ions on metallic targets.

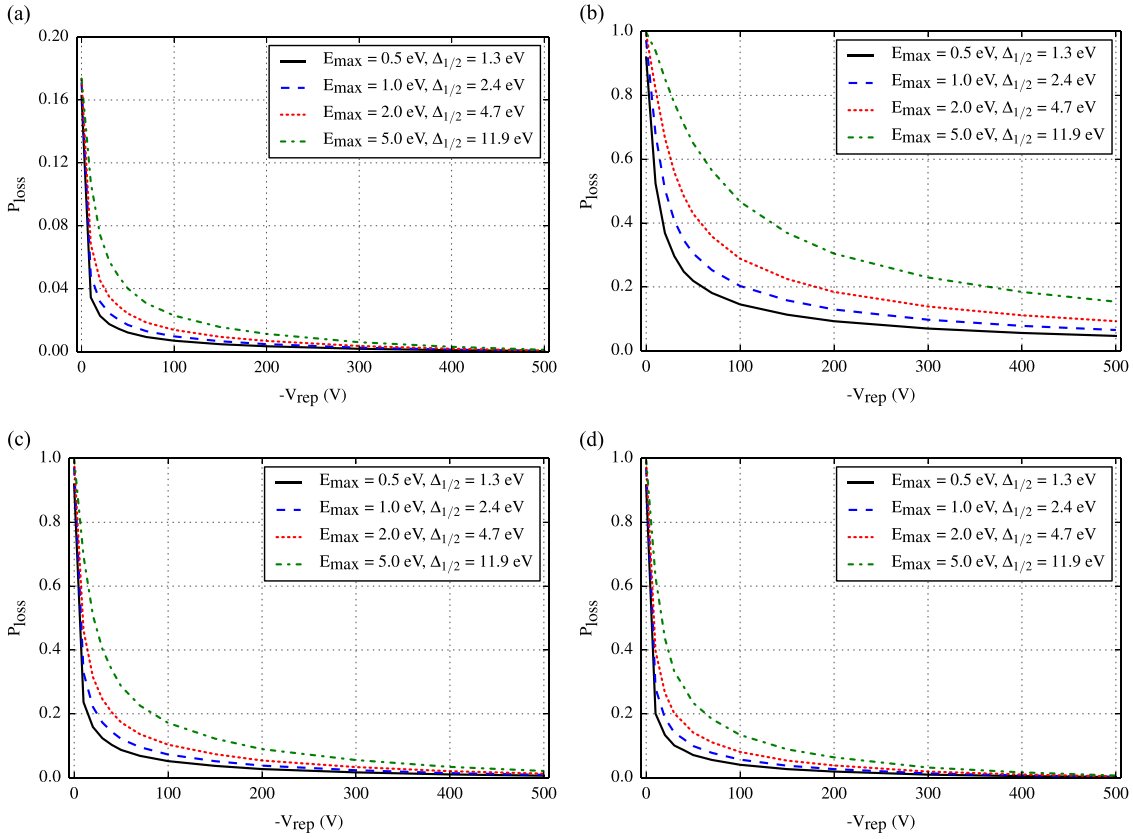

Fig. 13. Dependence of the electron loss probability P_{loss} on the repelling voltage V_{rep}, for the electron energy spectra shown in Fig. 12. (a) Results for REX-ISOLDE FC. (b) Results for prototype 1. (c) Results for prototype 2. (d) Results for final design.

considered for the studies on the dependence of P_{loss} on $N(E)$ using the calculated probabilities η of the four FCs. The results for the electron loss probabilities for such spectra are presented in Fig. 13.

The REX-ISOLDE FC with its typical design captures more than 80% of the emitted electrons due to its geometry. That is observed in Fig. 13a as for $V_{rep} = 0$ V, P_{loss} is lower than 0.17. The loss of electrons is highly reduced when biasing the repeller. For all the FCs by increasing the mean energy of the emitted electrons by an order of magnitude the probability of losing electrons P_{loss} is increased by a factor three for repelling voltages in the range $-V_{rep} = 100$–500 V. For the compact FCs and low repelling voltages, P_{loss} becomes larger and converges in all cases to $P_{loss} = 1$ for $V_{rep} = 0$ V, as expected due to the lack of walls on the collector, which implies that all emitted electrons are lost when no repelling fields are present in the cup.

References

[1] P. Strehl, Beam Instrumentation and Diagnostics, Springer, 2006. http://dx.doi.org/10.1007/3-540-26404-3.

[2] J. Harasimowicz, C.P. Welsch, L. Cosentino, A. Pappalardo, P. Finocchiaro, Physical Review ST Accelerators and Beams 15 (2012) 122801 http://dx.doi.org/10.1103/PhysRevSTAB.15.122801.

[3] M. Lindroos, P.A. Butler, M. Huyse, K. Riisager, Nuclear Instruments and Methods in Physical Research B 266 (2008) 4687 http://dx.doi.org/10.1016/j.nimb.2008.05.136.

[4] Y. Kadi, A.P. Bernardes, Y. Blumenfeld, S. Calatroni, R. Catherall, M.A. Fraser, B. Goddard, D. Parchet, E. Siesling, W. Venturini Delsolaro, D. Voulot, L.R. Williams. Status and future perspectives of the HIE-ISOLDE project at CERN, in: Proceedings of IPAC 2012, IPAC, 2012, pp. MOOBA02.

[5] D. Cantero, W. Andreazza, E. Bravin, A. Sosa, The status of beam diagnostics for the HIE-ISOLDE linac at CERN, in: Proceedings of IBIC 2014, IBIC, 2014, pp. WEPF13, pp. 565–568. ⟨http://www.slac.stanford.edu/econf/C140914/papers/wepf13.pdf⟩.

[6] D. Hasselkamp, S. Hippler, A. Scharmann, Nuclear Instruments and Methods in Physical Research B 18 (1987) 561. doi:110.1016/S0168-583X(86)80088-X.

[7] F. Hamme, U. Becker, P. Hammes, Simulation of secondary electron emission with CST Particle Studio, in: Proceedings of ICAP 2006, ICAP, 2006, pp. TUAPMP04.

[8] D. Habs, et al. The REX-ISOLDE project, Hyperfine Interactions, 129, 2000, pp. 43–66.http://dx.doi.org/10.1023/A:1012650908964.

[9] W.K. Chu, J.W. Mayer, M.A. Nicolet, Backscattering Spectrometry, Academic Press, Inc., New York, 1978.

[10] D. Hasselkamp, Kinetic electron emission from solids surfaces under ion bombardment, Springer Tracts in Modern Physics, vol. 123, 1992, p. 1 (Chapter 1) http://dx.doi.org/10.1007/BFb0038297.

[11] CST – Computer Simulation Technology. ⟨http://www.cst.com⟩.